

Revision of the paper for the proceedings of the ASTM Symposium on  
*Effect of Surface Coatings and Treatments on Wear*

**Friction and Wear of Self-Lubricating TiN-MoS<sub>2</sub> Coatings  
Produced by Chemical Vapor Deposition**

P. J. Blau, C. S. Yust, Y. W. Bae, T. M. Besmann, and W. Y. Lee  
Metals and Ceramics Division  
Oak Ridge National Laboratory  
P. O. Box 2008  
Oak Ridge, TN 37831-6063  
(615) 574-5377; FAX (615) 574-6918

RECEIVED

DEC 08 1995

## Abstract

OSTI

The purpose of the work reported here was to develop special chemical vapor deposition (CVD) methods to produce self-lubricating ceramic coatings in which the lubricating and structural phases were co-deposited on Ti-6Al-4V alloy substrates. These novel composite coatings are based on a system containing titanium nitride and molybdenum disulfide. The method for producing these coatings and their sliding behavior against silicon nitride counterfaces, in the temperature range 20 -700° C in air, are described. The initial sliding friction coefficients for the composite coatings at room temperature were 0.07-0.30, but longer-term transitions to higher friction occurred, and specimen-to-specimen test variations suggested that further developments of the deposition process are required to assure repeatable friction and wear results. Friction and wear tests at 300 and 700° C produced encouraging results, but tests run at an intermediate temperate of 400° C exhibited friction coefficients of 1.0 or more. Oxidation and a change in the nature of the debris layers formed during sliding are believed to be responsible for this behavior.

Key words: friction, wear, chemical vapor deposition, titanium nitride, coatings, molybdenum disulfide, self-lubricating materials

## Introduction

Coatings and surface treatments represent important strategies for affecting friction and wear improvements on load-bearing, sliding surfaces. There are a large number of such treatments currently available.<sup>1,2,3</sup> In fact, entire journals are devoted to the subject.<sup>4</sup> Coating processes involve adding material to the surface. Others treatments, like ion-implantation and diffusion treatments, involve modifying the composition and/or structure of the materials at and just below the surface.

Materials which contain an additive or additives which reduce friction during use are called self-lubricating materials. Examples of self-lubricating materials include polymer blends which contain tetrafluoroethylene and porous, oil-impregnated bronzes. Self-lubricating materials are useful for a number of reasons:

1. They can serve as fail-safe protection in a liquid lubricated system in case the liquid lubricant is lost or fails for some other reason.
2. They can lubricate parts of machinery where it is not practical to use external lubrication supply systems.

"The submitted manuscript has been authored by a contractor of the U.S. Government under contract No. DE-AC05-84OR21400. Accordingly, the U.S. Government retains a nonexclusive, royalty-free license to publish or reproduce the published form of this contribution, or allow others to do so, for U.S. Government purposes."

DISTRIBUTION OF THIS DOCUMENT IS UNLIMITED

MASTER

3. They can operate in severe environments, such as high-temperatures, where liquid lubricants may not work.
4. They can be sealed into assemblies which must function effectively without having the opportunity to add more lubricant.
5. They may be a cost-effective alternative to other lubrication schemes.

In the present context, a self-lubricating coating consists of a matrix phase to provide a measure of wear resistance and load-bearing structure, and a solid lubricating phase to reduce friction. The coating should be so constructed such that there is sufficient quantity of lubricant to spread over the surface, yet not so much that the coating becomes too soft to support the load or to retain its integrity and adhesion to the substrate. In the ideal case, the wear of the coating should be low and just sufficient to continue to supply additional lubricating phase to the surface to replenish that which is lost by wear or transfer to the opposing surface.

For the matrix phase, we selected titanium nitride, a ceramic material whose success as a wear-resistant coating material for tooling and other tribological applications is well-established. For the lubricating phase, we selected molybdenum disulfide, a solid lubricating material with moderate elevated temperature capabilities. At temperatures of approximately 350–400°C, MoS<sub>2</sub> tends to oxidize to form MoO<sub>3</sub>.<sup>5</sup> The challenge of this effort was to simultaneously deposit the matrix and lubricating phases by controlled CVD so as to produce a functional coating.

Results of earlier microfriction studies indicated that the method of applying MoS<sub>2</sub> to surfaces affects the stability and nominal value of the friction coefficient when sliding against silicon nitride.<sup>6</sup> The current work presents results of sliding friction and wear tests of our composite coatings against silicon nitride which were conducted in air at temperatures between about 20 and 700° C.

### Coating Synthesis and Characterization

Deposition of composite coatings of TiN-MoS<sub>2</sub> was carried out on polished Ti-6Al-4V alloy substrates in a cold-wall CVD reactor at 1073 K and a system pressure of 5.3 kPa. The precursor gases were composed of tetrakis (dimethylamino) titanium, Ti((CH<sub>3</sub>)<sub>2</sub>N)<sub>4</sub>, (99.9 %, Strem Chemicals Inc., Newburyport, MA), MoF<sub>6</sub> (99.9 %, Johnson & Matthey, Wardhill, MA), NH<sub>3</sub> (99.95 %, Alphagaz, Morrisville, PA), and H<sub>2</sub>S (99.5 %, Alphagaz). The reaction chamber, constructed of a fused silica tube, was 61 cm long and 3.3 cm in inner diameter. Stainless steel flanges with compression O-ring fittings were used to seal the reactor assembly at both ends. Mass flow controllers were used to control gas flows, and the system pressure was controlled by using a mechanical pump with a solenoid flow valve coupled with a pressure controller and a capacitance manometer.

150 g of Ti((CH<sub>3</sub>)<sub>2</sub>N)<sub>4</sub> was contained in a 200-cm<sup>3</sup> bubbler maintained at a constant temperature of 338 K using a silicon oil bath with an immersion circulator. The vapor pressure of Ti((CH<sub>3</sub>)<sub>2</sub>N)<sub>4</sub> at this temperature is  $\approx$  200 Pa.<sup>7</sup> Ar at 20 cm<sup>3</sup>/min at STP was passed through the bubbler to carry the vapor into the reactor. The flow rate of NH<sub>3</sub> was 300 cm<sup>3</sup>/min at STP which was separately fed into the reaction zone using a dual-path, co-axial injector made of Inconel to prevent premature reaction with the Ti precursor. The flow rates of MoF<sub>6</sub> and H<sub>2</sub>S were 6 and 60 cm<sup>3</sup>/min at STP, respectively. The Ti alloy substrates (1.8 cm x 2.5 cm) were placed on a 13-cm long graphite susceptor which was inductively heated by a radio frequency field (164 kHz). A K-

type thermocouple in contact with the graphite susceptor was used to measure temperatures. Film thicknesses of 3 - 4  $\mu\text{m}$  were produced.

X-ray diffraction patterns such as that shown in Fig. 1 were obtained on the TiN-MoS<sub>2</sub> composite coatings to determine their structures and compositions. Peaks marked with asterisks in the figure arose from the substrate. While no preferred orientation was predominant in the case of TiN, MoS<sub>2</sub> was found to be textured such that its (002) planes were aligned parallel to the coating surface. This orientation is highly desirable to produce maximum lubricity. The deposition rate, estimated from the coating cross-sections analyzed by electron microprobe analysis, averaged  $\approx 10 \mu\text{m/h}$ . Studies using Auger electron spectroscopy (AES) indicated that the MoS<sub>2</sub> content in the TiN-MoS<sub>2</sub> composite coatings increased as a function of the coating thickness. Selected-area, electron diffraction analysis indicated that the coating surface was primarily MoS<sub>2</sub>, and both TiN and MoS<sub>2</sub> were identified near the substrate, in agreement with the results obtained by the AES analysis. A transmission electron micrograph of the composite coating in the transverse direction showed that MoS<sub>2</sub> was present as pockets dispersed in a matrix consisting of  $\approx 50\text{-nm}$  TiN crystallites (see Fig. 2).

### Friction and Wear Testing Procedure

Friction and wear testing was performed in a high-temperature pin-on-disk tribometer which is capable of continuous rotation in either clockwise or counter clockwise directions, or of oscillation over a specified angular range. The latter mode was used for these experiments. The pin specimen, in these tests a 9.53 mm diameter silicon nitride (NBD200) sphere, was held in the end of a rod anchored in a strain-gaged collar arrangement which allowed recording both the normal and tangential forces during the test. The pin holder and the disk rotation system move along a vertical axis, bringing the pin and the disk into contact at the center of a resistance heated furnace. The furnace heating element is contained within quartz tubes, the outermost tube being gold-coated for reflection of radiation. A schematic illustration of the test configuration is shown in Fig 3.

The present tests were done using oscillatory motion over an arc of 90 degrees. The oscillation frequency was 40 cycles/min and the wear track diameter was 20 mm. The resultant average sliding velocity was approximately 20 mm/s. An applied force of 16.4 N was selected in order to provide an elastic, Hertzian contact pressure of 1 GPa for the silicon nitride sphere on the titanium alloy plane at the given test temperature. In one low-load test, the applied force was reduced to 1 N (0.37 GPa). The standard test duration was 500 cycles (12.5 min); however, additional tests of up to 4 hrs in duration examined the effect of more prolonged sliding. Tests were performed at room temperature and at temperatures up to 700° C. Ambient atmosphere was used in all the tests.

Tangential force and normal force were periodically sampled by a computer-driven data acquisition system. Data were recorded for 30 seconds at two-minute intervals at a rate of 125 s<sup>-1</sup> during the 500-cycle tests, and at selected periods during more extended tests. A strip chart recorder was also used to display the general trend of both tangential and normal force in all tests. The figures depicting friction coefficient as a function of time presented here are all based on the computer-recorded data. The coatings and conditions used for these experiments are listed in Table 1.

### Results of Friction and Wear Tests

Room Temperature Tests. Friction results for the room temperature tests are given in Table 2 and Fig. 5. The first three rows of Table 2 contain baseline data for a polished Ti-6Al-4V specimen, a TiN coating and a MoS<sub>2</sub> coating (500 cycles, 12.5 min.). As shown in Fig. 4, the

friction coefficient for the bare substrate began at 0.55, decreased to 0.4 after 2 minutes of sliding, and remained at this value for the remainder of the test. The wear track was 10  $\mu\text{m}$ -deep (by profilometric measurement) with displaced material displaying deformation twinning at the track edge, as shown in Fig. 5. The tip of the slider was covered by adherent debris.

The friction coefficient of the TiN-coated specimen rose from 0.5 to 0.8 after only 5 minutes of sliding. The only evidence of wear was the flattening of the coating surface in the wear path caused either by the removal of prominent summits of the profile and/or filling of some of the profile valleys with wear debris. Figure 6 shows the highly-fractured appearance of the track surface. A debris-free wear flat 715  $\mu\text{m}$  in diameter was formed on the slider tip, suggestive of abrasive wear by the hard TiN coating.

The friction coefficient in the MoS<sub>2</sub> coating test remained at about 0.2 for the entire 500 cycles, but on the 4 hr. test reached 0.32. Because the starting film was about twice the thickness of the other coatings (8  $\mu\text{m}$ ), there was more material available to form a lubricating transfer film on the slider tip, and its effect lasted relatively long.

Composite coating specimens containing both TiN and MoS<sub>2</sub> were produced. Five tests of 500 cycles duration were conducted. The initial friction coefficients increased from about 0.07-0.20, in the first two minutes, to 0.13 to 0.22 for the remainder of the tests. In some specimens, the friction coefficient remained relatively low, but in others, it was higher and varied considerably during the test. Figure 7 shows the relatively smooth appearance of the wear track of one of the composite coating specimens which gave low friction results.

A longer run was conducted on the composite coating to investigate the effects of coating wear-through. The run was terminated at 3.83 h when there was clear evidence for wear-through (i.e., transition to a high, erratic friction coefficient and a change in the appearance of the wear track). The structure of the wear track exhibited three zones: (1) a zone covered with dark patches at the center of the track, (2) a zone partially covered with residual coating material to each side of it, and (3) a narrow band suggestive of a still intact portion of the coating by the track edge (see Fig. 8). A profile of the wear track is shown in Fig. 9. The friction force record of this run exhibited an increasing trend as the proportion of the track width covered by the intact coating continued to decrease.

### Elevated Temperature Test Results

Coatings were tested at temperatures of 300, 400, and 700° C in air. Results are shown in Fig. 10. Tests at 300° C behaved similarly in friction and wear to those run at room temperature. Tests at 400° C, however, did not produce the same low friction and wear. The same specimen which exhibited friction coefficients from 0.1 to 0.14 at room temperature was tested at 400° C in an air atmosphere. The initial friction coefficient value was 0.35, but it increased very rapidly to 0.62 at the end of 1 minute and reached a final value of 0.75 at 12.5 min. To assess the possibility that lower friction coefficients would obtain under reduced contact stress, this coating was tested again at 400° C, but at 1 N applied normal force (0.37 GPa). The initial friction coefficient was 0.7 and it increased continually to reach 1.0 at the end of the 12.5 min test. Despite the difference in initial friction values, the elevated temperature response of the coating in two tests was similar, as shown in Fig. 11. Relatively debris-free wear flats, surrounded by some adhered debris, were formed in both 400° C tests. A final run was conducted at 700° C. Friction coefficients for this run were lower than those for the 400° C.

## Discussion

A primary issue involved in developing any new tribological surface treatment or coating is that of performance repeatability. Three tests with the same load, speed, and duration were performed on the same specimen, but friction and wear results were not similar, suggesting place-to-place variations in the composition or microstructure within a given coating. Visual inspection of the coating surfaces indicated the likelihood of this variability (e.g., a nodular appearance in some regions, powdery appearance in others). Auger analysis and depth profiling of the composite coatings indicated that the MoS<sub>2</sub> content decreased with depth. This composition gradient probably contributed to the increase in friction as the coatings wore.

Studies of the friction versus time records for the room temperature coating tests, including the longer duration runs, revealed that friction force tended to follow a complex series of changes before reaching what might be termed the steady-state condition. Friction curve analysis is an established method to assess the repeatability of test conditions as well as the uniformity of the starting materials and scheme of lubrication.<sup>8</sup> A commonly-observed behavior in the coating tests would be for the friction force to climb rapidly at first, level off, experience a sharp drop, and finally rise to a steady-state value. Steady-state, in the present sense, involved considerable fluctuations in friction force about a mean value. Other types of frictional variations were also observed, reinforcing the idea that the composition and microstructure of the coatings varied from place-to-place on the specimens. This suggests a sequence of evolving interfacial processes: initial abrasion and transfer of material to the slider, smoothing of the as-formed coating features, texturing of the surface layers, and finally, gradual break-through to expose the substrate below. Even when the substrate was exposed, microscopic evidence suggested that some residual coating material, mixed with wear debris, remained on the wear track to modify its frictional behavior.

Elevated temperature friction results were encouraging for high and low temperature tests but not for intermediate temperatures. Friction coefficients were low at 300° C and relatively low at 700° C, but not at 400° C. At 400° C, friction coefficients quickly rose to unacceptably high levels ( $\mu \approx 0.8 - 1.0$ ). It was hoped that tying the MoS<sub>2</sub> up in a very fine-grained composite with TiN might help retain its lubricating qualities at the higher temperatures, but in light of the current results, is suspected that the MoS<sub>2</sub> was oxidized to form MoO<sub>3</sub>, a compound not known to be an effective lubricant.

The decrease in friction at 700° C is encouraging for higher temperature applications. It might initially be suspected that TiO<sub>2-x</sub>, a candidate solid lubricant, might have helped reduce the friction at 700° C, but earlier results from Gardos on the friction of rutile single crystals at various temperatures and partial pressures indicated that friction coefficients of about 0.6-0.8 were typical of that material in air at 700° C.<sup>9</sup>

No chemical analysis data were available for the high-temperature wear-tested specimens, and the specific composition of the wear surface layers from the elevated temperature tests must remain for future study. Nevertheless, there is good reason to suspect that the tribochemistry of the elevated temperature wear surfaces was a major influence in the coating behavior. In particular, the formation of lubricious oxides on the surface is known to reduce sliding friction in metals and some ceramics, however, it is not clear that such oxides, once formed, would resist wear very well.

Finally, a comment should be made regarding the type of tests used to evaluate these coatings. The contact conditions in the present experiments were relatively severe (ball-on-flat). It is possible that the composite coatings would perform better in a conformal contact situation, like a that of journal bearing, face seal, or bushing. Thus, the current results suggest that the coatings

may not be appropriate for highly-concentrated sliding conditions as might occur in non-conformal contacts unless improvements in homogeneity are made through further process development.

### Summary and Conclusions

Composite, self-lubricating coatings have been produced by CVD on titanium alloy substrates. The coatings contained very fine-grained mixtures of TiN and MoS<sub>2</sub>. The composite composition seemed to adhere better compared to MoS<sub>2</sub> CVD coatings alone. While low initial friction coefficients (0.07-0.20, typically) were obtained against silicon nitride sliders, longer-term behavior was quite variable. The latter result is attributed to coating heterogeneity, a subject which needs to be addressed in future development of this coating system.

Friction force-time traces indicate that the wear-through of the coating usually is not an instantaneous event, but rather progresses through a series of stages. Thus, the benefits of the lubrication with the coating persist even when some of the substrate has been exposed.

While the composite coatings show promise for room and elevated temperature applications at 300° and 700° C, test results at 400° C indicate that use at this temperature is not favored from a high-friction standpoint. Differences in the oxide compositions and the debris layers formed at different temperatures are suggested as the reason for this behavior. In particular, the formation of lubricious oxides may reduce friction coefficients at 700° C, but experimental validation of this hypothesis and data on the durability of the oxide films at that temperature have yet to be obtained.

### Acknowledgments

This research was sponsored by the Department of Energy, Division of Advanced Energy Projects, under contract DE-AC05-84OR21400 with Martin Marietta Energy Systems, Inc. The authors wish to thank the internal reviewers at Oak Ridge National Laboratory for their useful comments on this manuscript.

---

### DISCLAIMER

This report was prepared as an account of work sponsored by an agency of the United States Government. Neither the United States Government nor any agency thereof, nor any of their employees, makes any warranty, express or implied, or assumes any legal liability or responsibility for the accuracy, completeness, or usefulness of any information, apparatus, product, or process disclosed, or represents that its use would not infringe privately owned rights. Reference herein to any specific commercial product, process, or service by trade name, trademark, manufacturer, or otherwise does not necessarily constitute or imply its endorsement, recommendation, or favoring by the United States Government or any agency thereof. The views and opinions of authors expressed herein do not necessarily state or reflect those of the United States Government or any agency thereof.

---

## References

---

- 1 "Surface Treatments and Coatings for Friction and Wear Control," in ASM Handbook, 10<sup>th</sup> edition, Vol. 18, Friction, Lubrication, and Wear Technology, ASM International<sup>TM</sup>, Materials Park, Ohio, 1992, pp. 829-883.
- 2 Budinski, K. G., Surface Engineering for Wear Resistance, Prentice Hall, Englewood Cliffs, NJ, 1988.
- 3 Peterson, M. B. and Ramalingam, S., "Coatings for Tribological Applications," in Fundamentals of Friction and Wear of Materials, ASM, Materials Park, Ohio, 1981, pp. 331-372.
- 4 Surface Coatings and Technology, Elsevier Sequoia, Lausanne, Switzerland.
- 5 Lancaster, J. K., "Solid Lubricants," in CRC Handbook of Lubrication, Vol. II, ed. E. R. Booser, CRC Press, Boca Raton, Florida, 1983, pp. 269-286.
- 6 Blau, P. J. and Yust, C. S., "Microfriction Studies of Model Self-lubricating Surfaces," Surface and Coatings Technology, Vol. 62, 1993, pp. 380-387.
- 7 A. Katz, A. Feingold, S.J. Pearton, S. Nakahara, M. Ellington, U.K. Chakrabarti, M. Geva, and E. Lane, J. Appl. Phys., 70[7], 1991, p. 3666.
- 8 P. J. Blau, "Shapes and Other Attributes of Friction Break-in Curves," in Friction and Wear Transitions in Materials, Noyes Publications, Park Ridge, New Jersey, 1992, pp. 271-288.
- 9 M. N. Gardos, H.-S. Hong, and W. O. Winer, "The Effect of Anion Vacancies on the Tribological Properties of Rutile (TiO<sub>2-x</sub>), Part II: Experimental Evidence," Tribology Trans., Vol. 22 (2), 1990, pp. 209-220.

**Table 1. FRICTION AND WEAR TESTS PERFORMED IN THIS STUDY**

Composition	Temp. (°C)	Test Time (min)	Number of Tests
polished Ti-6Al-4V alloy	20	12.5	1
TiN-rich coating	20	12.5	1
CVD MoS <sub>2</sub> coating	20	12.5	1
" "	20	240.	1
composite TiN-MoS <sub>2</sub> coating	20	12.5	5
" " "	20	61.	1
" " "	20	90.	1
" " "	20	120.	1
" " "	20	230.	1
" " "	300	12.5	1
" " "	400	12.5	2
" " "	700	12.5	1

**Table 2. FRICTION RESULTS: ROOM TEMPERATURE TESTS**  
(all tests at 1 GPa contact pressure, reciprocating, in air)

Composition	$\mu$ initial	Trend in $\mu$	$\mu$ final
uncoated substrate	0.44	rapid decrease	0.40
TiN-rich coating	0.50	rising	0.80
MoS <sub>2</sub> coating	0.18-0.21	rising, highest for the 4 hr test	0.20/0.32
Composite coating (12.5 min tests)	0.07-0.20	rise/drop/rise behavior was common	0.13-0.22 (0.6 for Run 114)
Composite coatings (>60 min tests)	0.09-0.30	rise/drop/rise behavior was common	0.40-0.60

**Table 3. WEAR TRACK DEPTHS FOR ROOM TEMPERATURE TESTS**

Disk Specimen	Test Time (min.)	Approximate Track Depth ( $\mu$ m)
Ti alloy	12.5	10.
MoS <sub>2</sub>	12.5	20.
TiN-MoS <sub>2</sub> coating	12.5	1.0
TiN-MoS <sub>2</sub> coating	120.0	40.

## Figure captions

Figure 1. X-ray diffraction pattern of the TiN-MoS<sub>2</sub> coating deposited on Ti-6Al-4V alloy substrate.

Figure 2. A transmission electron micrograph in the transverse direction of the TiN-MoS<sub>2</sub> composite coating.

Figure 3. Schematic diagram of the high-temperature tribometer. A. ball specimen, B. flat specimen, C. base plate for flat specimen stage, D. mounting rod for ball specimen, E. dead weight, F. resistance heating coils, G. gold-coated reflector, H. insulating plate, I. water cooling for the base plate, J. drive motor, K. aluminum base plate for the machine, L. glass bell jar.

Figure 4. Summary of friction data from room temperature tests of various coatings. Run numbers correspond to the data in Table 1.

Figure 5. Photomicrograph of a wear track on the Ti-6Al-4V substrate material showing deformation twinning at the track edge and periodic features within the grooves.

Figure 6. Fractured area on the surface of the TiN-coated specimen.

Figure 7. Smooth features on the composite coating surface.

Figure 8. Optical micrograph of the wear track for a 230 minute-long test showing three distinct regions.

Figure 9. Stylus profile (2 μm tip radius) of the wear track shown in Fig. 9.

Figure 10. Friction results for coatings tested at various temperatures. Symbol key: squares containing crosses = 20° C tests, triangles = 300° C tests, open squares = 400° C tests, and closed circles = 700° C tests.

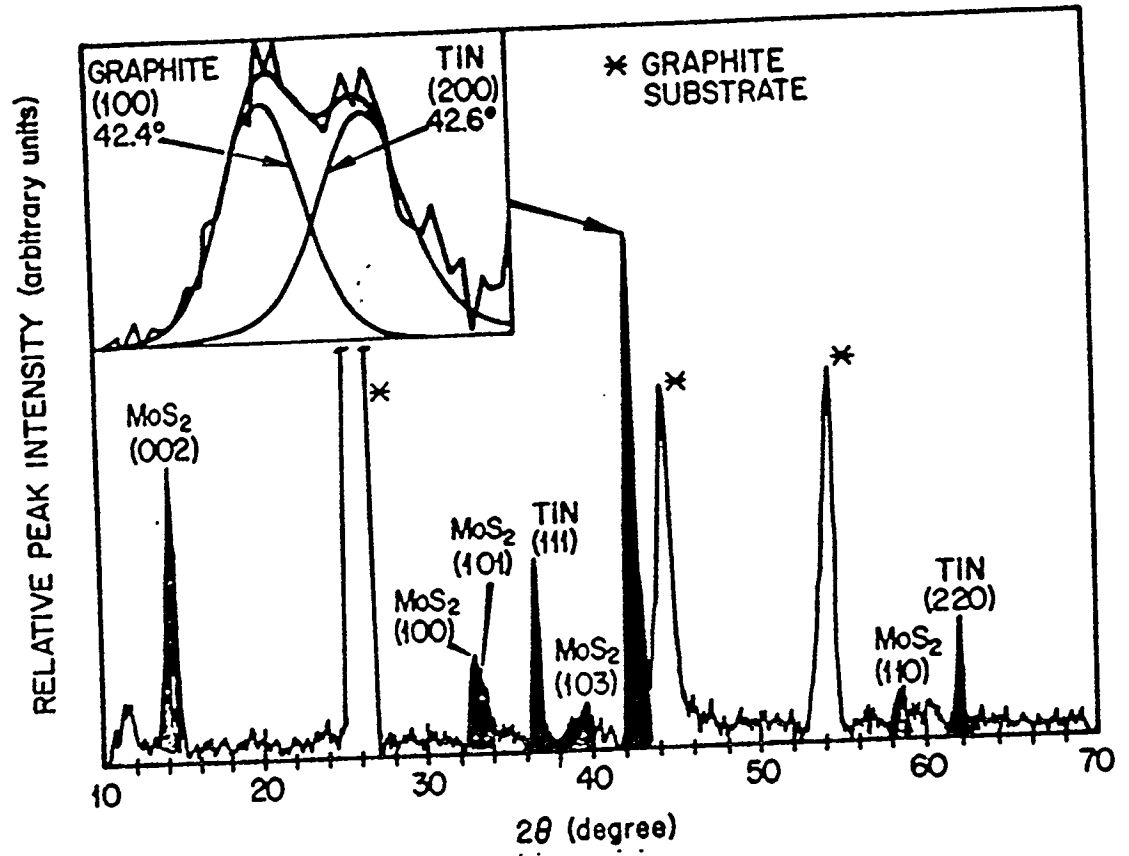


Fig. 1.

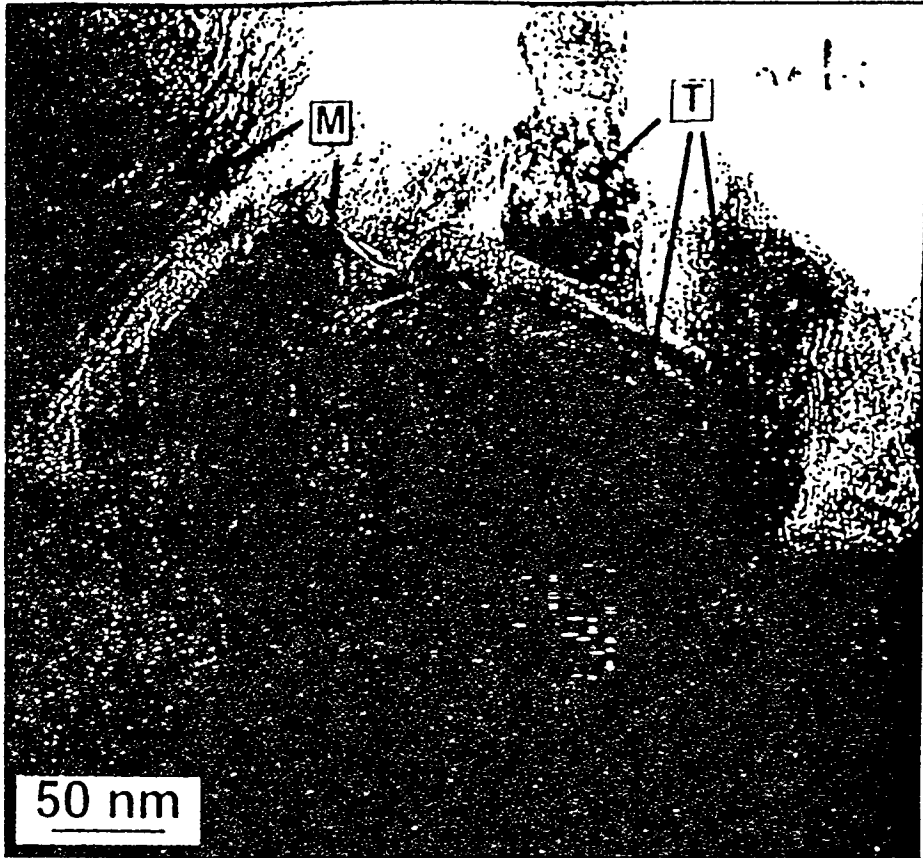


Fig. 2

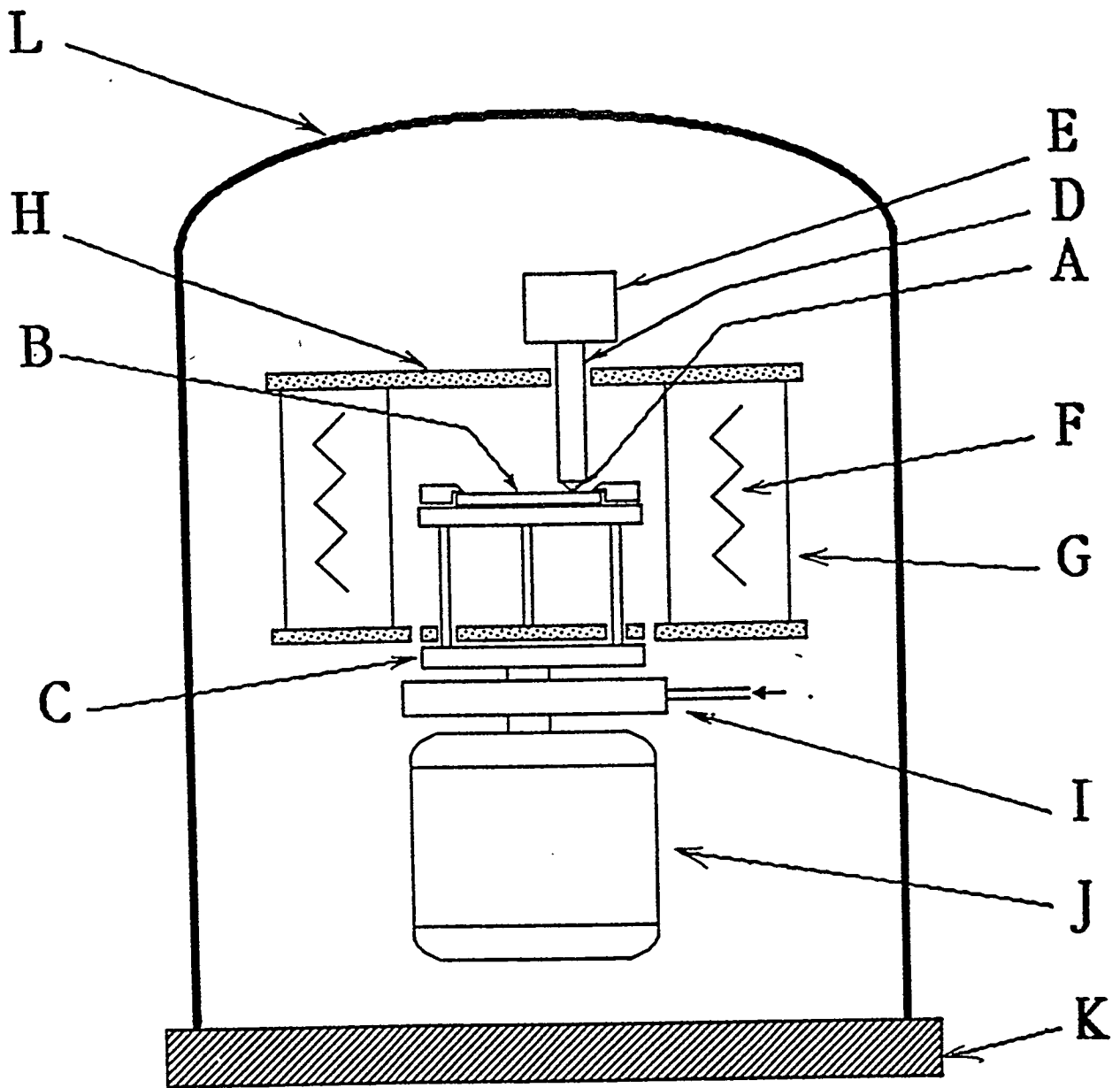


Fig. 3.

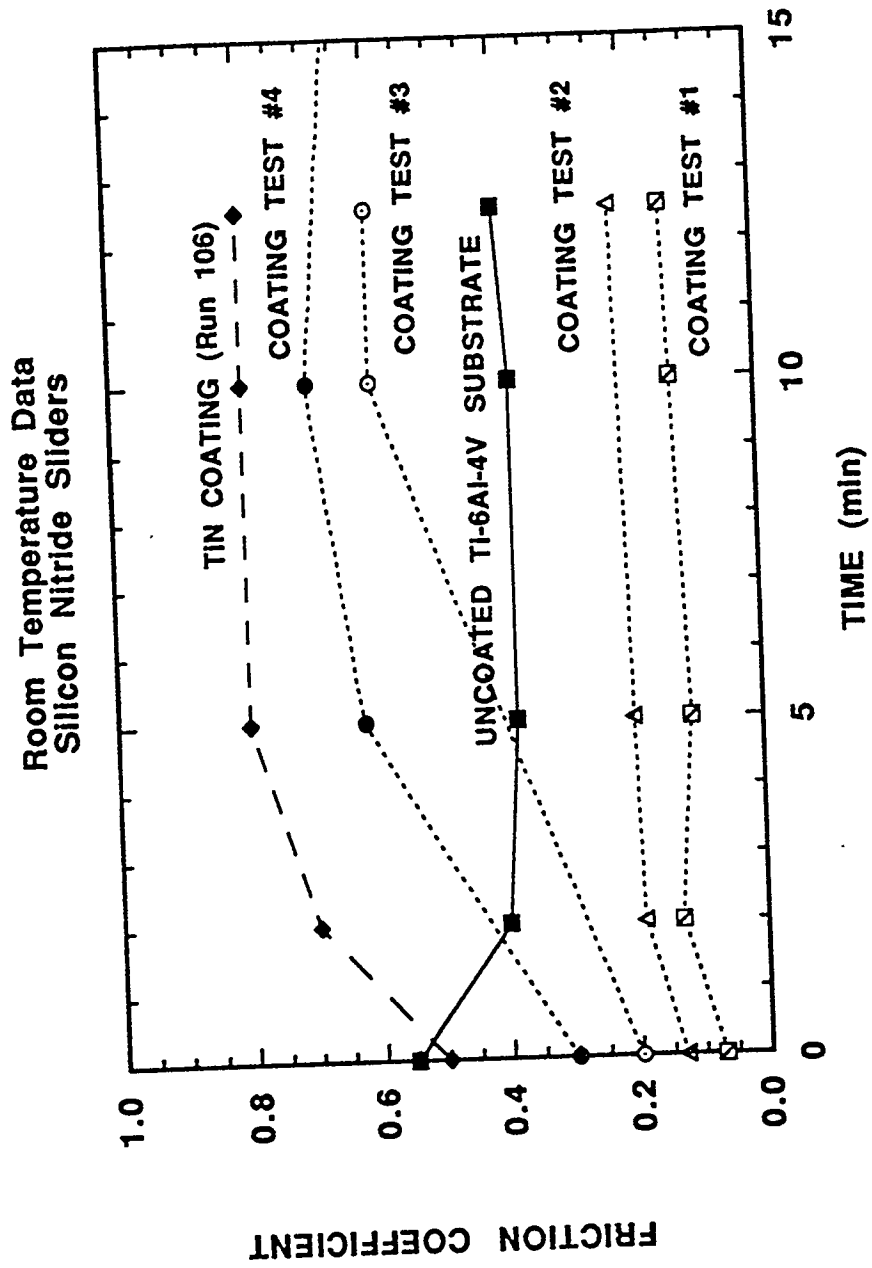


Fig. 4

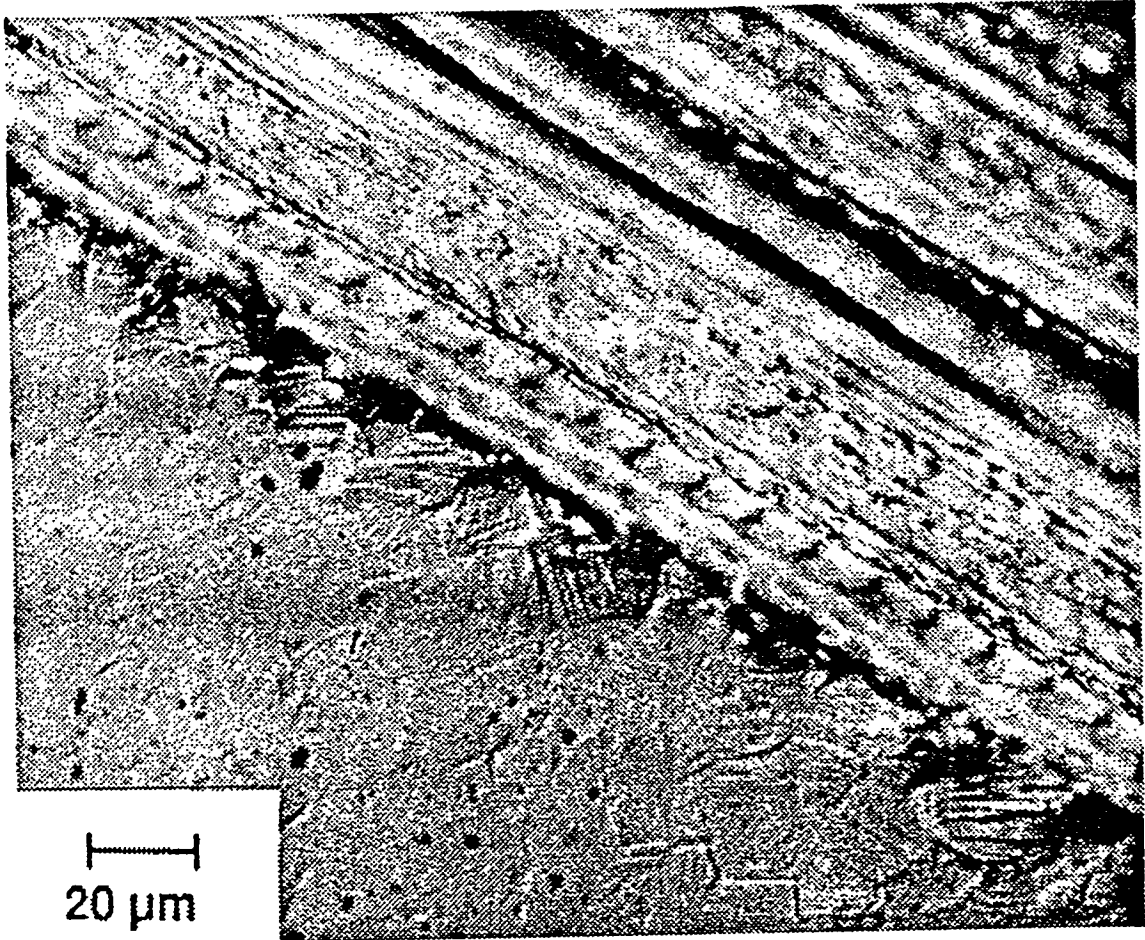


Fig 5

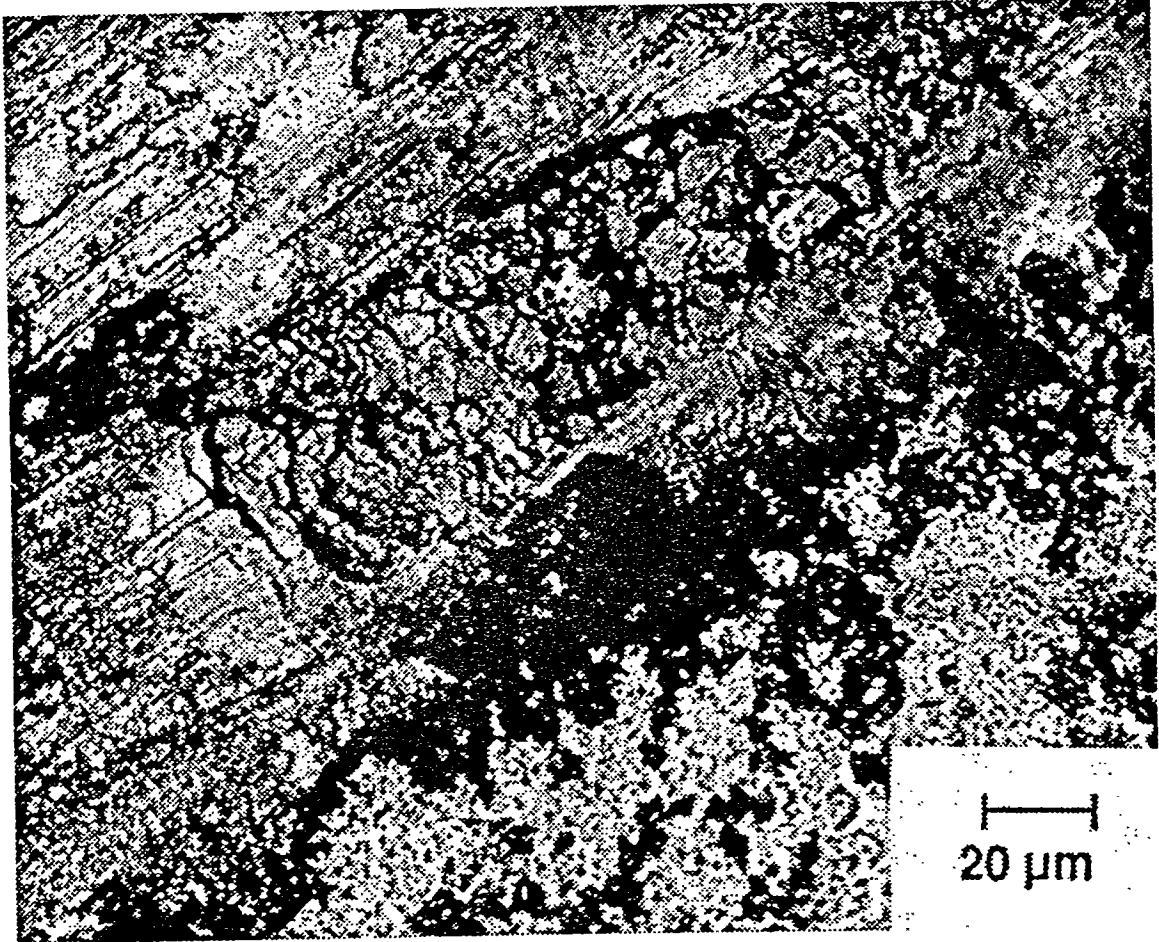


Fig 6

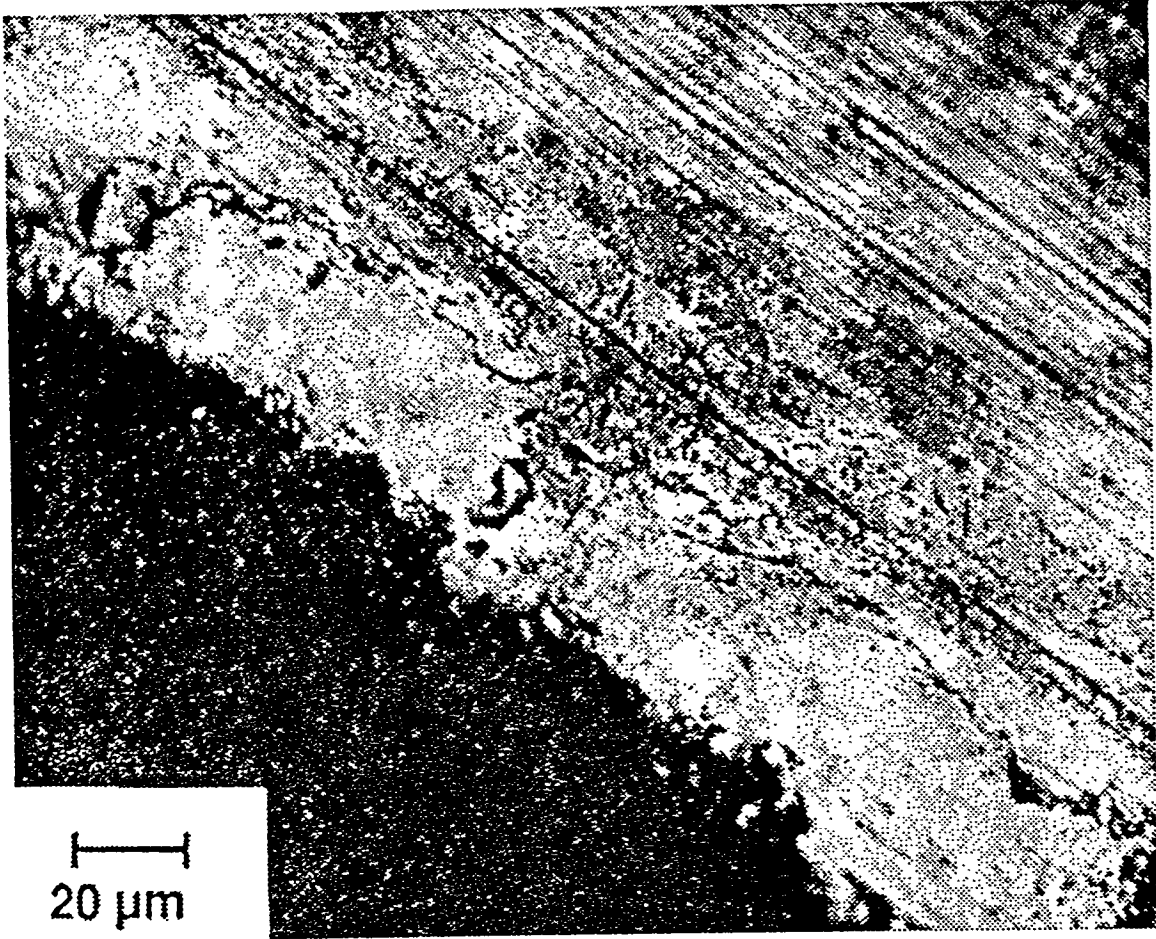
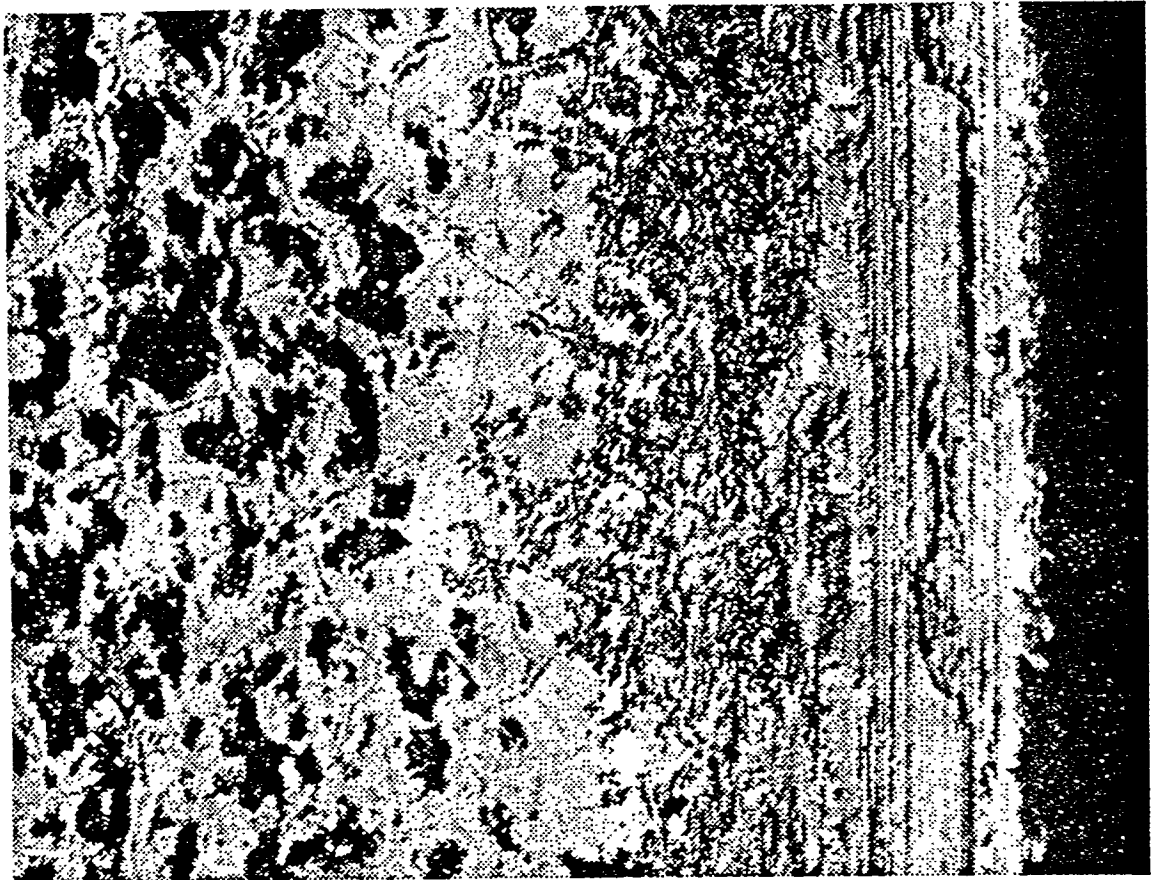


Fig 7



PATCHES OF DEBRIS

RESIDUAL  
COATING  
MATERIAL

WORN  
COATING

UNWORN  
COATING

10  $\mu\text{m}$

Fig. 8

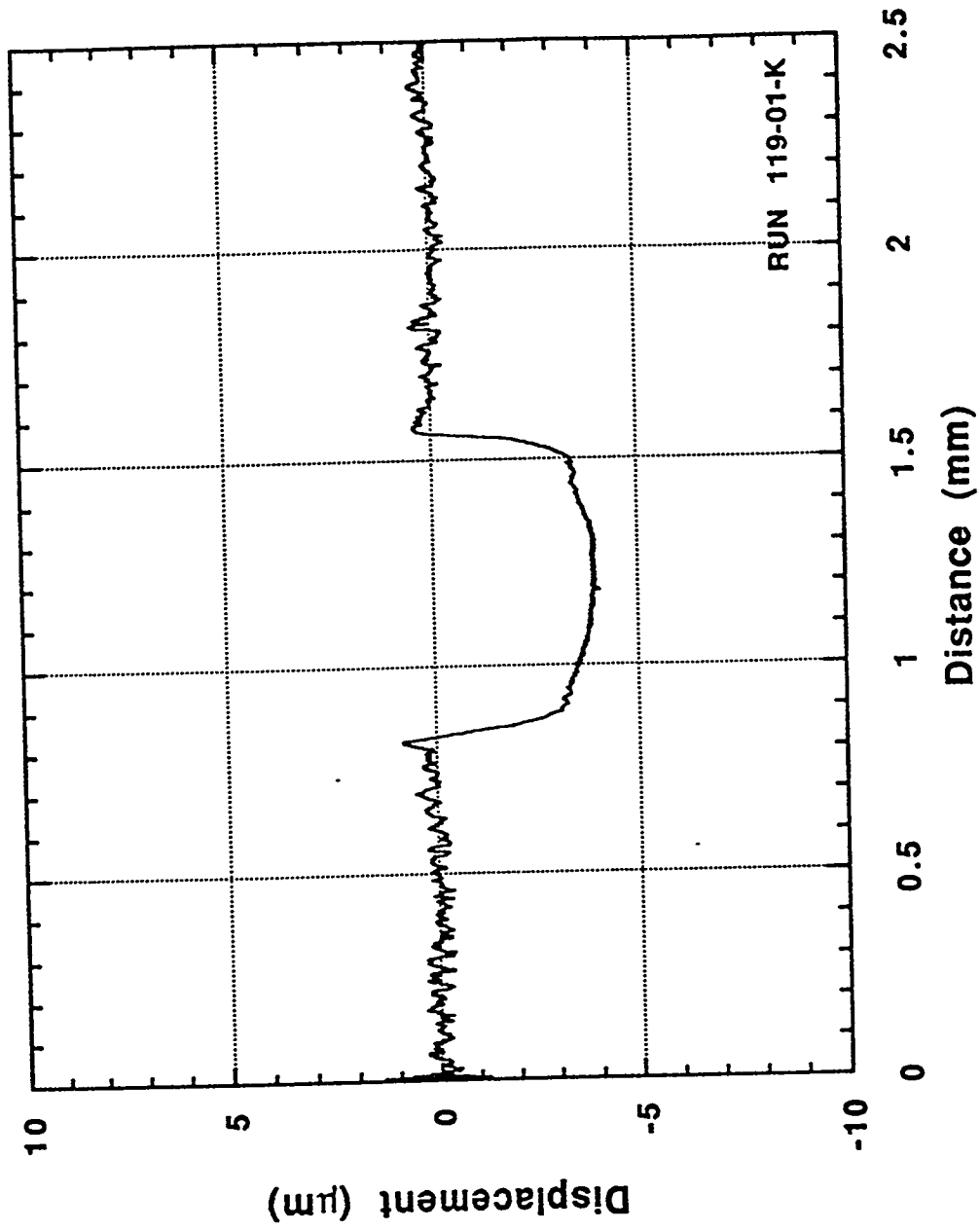


Fig. 9

# ELEVATED TEMPERATURE FRICTION RESULTS

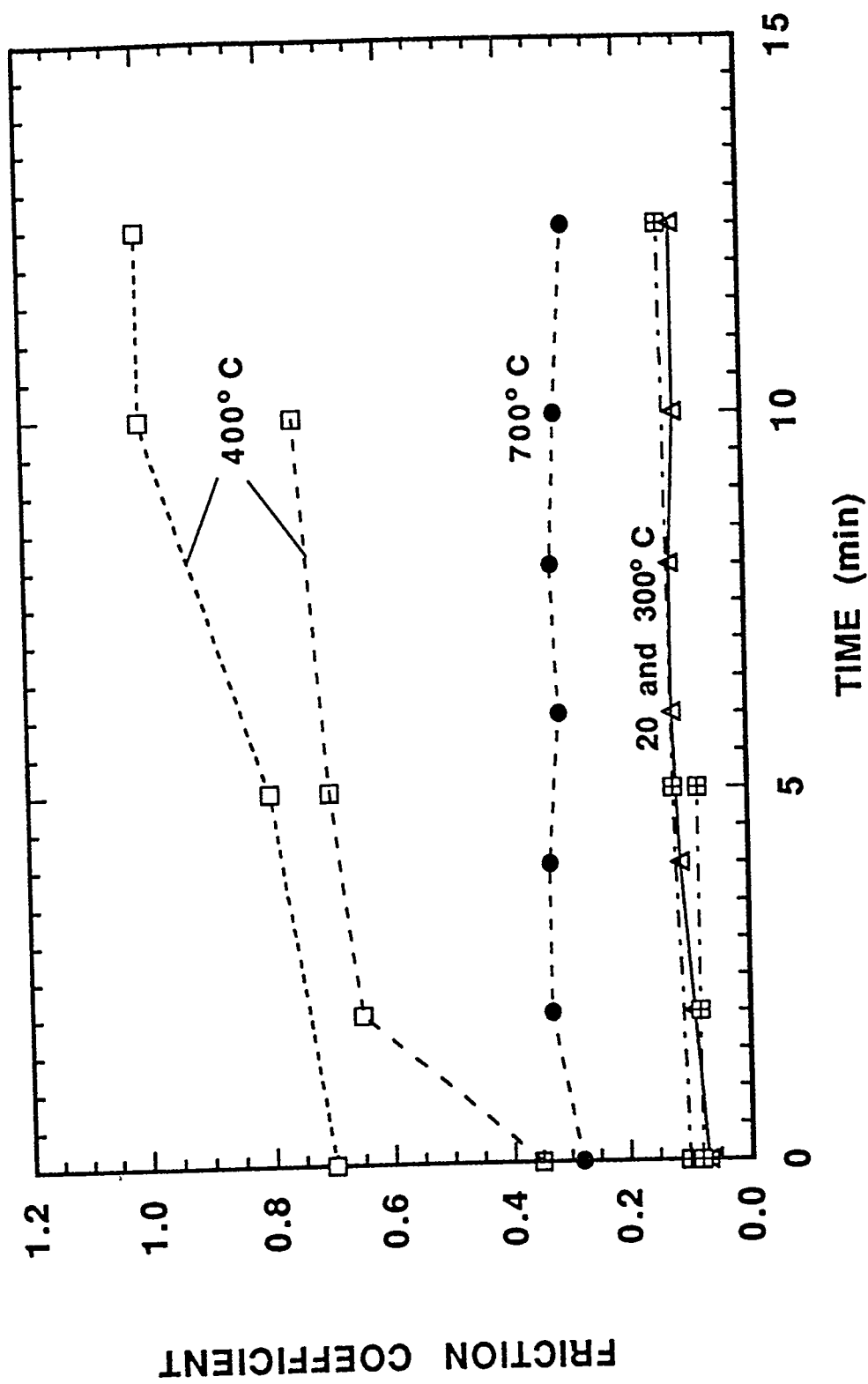


Fig. 10